"The Impossible Project" -

How to do a perfect SAXS measurement

Brian R. Pauw*

April 6, 2011

*Project co-workers: Hiroki Ogawa, Takumi Takano

Contents

Chapter 1

Introduction to small-angle scattering

1.1 What is this?

This document explains how to collect enough information during a SAXS experiment in order to be able to get most out of your data. A checklist is also provided to aid in ensuring that all necessary information is there. A second (future) part will discuss what to do after the perfect dataset has been collected, and shall thus focus on the data fitting procedures and models.

1.2 Introduction to SAXS

1.2.1 For who is this section intended?

If you are unfamiliar with the technique of SAXS, or have been asked to help out at a SAXS beam-time or experiment without too much prior knowledge, this section will provide a short introduction to SAXS. This section is an adaptation of the SAXS introduction available (besides other useful information) at `http://www.lookingatnothing.com/`. While the introduction that follows is not complete and contains many gaps in the details, it may provide a basis for understanding on which to continue building the knowledge. In other words, rather than to explain every aspect in detail before giving the overview

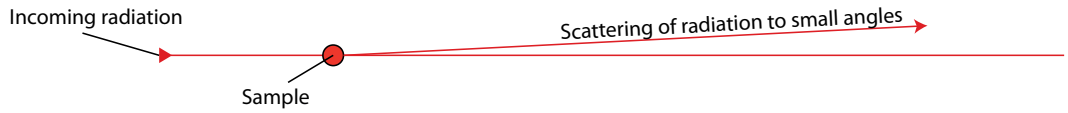

Figure 1.1: *Small angle scattering is the scattering of radiation to small angles by a sample.*

of how these aspects interact to form the technique, a rough introduction is given which will be fine-tuned later.

1.2.2 Welcome to SAS

Welcome to small-angle scattering. Techniques such as light scattering (LS), small-angle x-ray scattering (SAXS) and small-angle neutron scattering (SANS) are all small angle scattering techniques. These techniques are used to analyze the shape and size of objects much smaller than can be seen by eye, by analyzing the way that radiation (light, x-rays or neutrons) is scattered by the objects (c.f. Figure 1.1). The sizes we are talking about range from 1 micrometer to several angstrom (1 angstrom is 1×10^{-10} meters, or 0.0000000001 meter). One particular reason for choosing scattering over microscopic techniques is that a small-angle scattering measurement generally becomes easier to perform for smaller objects. There are other marked differences with microscopy, which will be discussed after a short explanation of the technique itself.

All aforementioned scattering techniques operate on the principle of wave interference when contrasting features are encountered in the sample. No photon energy loss is assumed in most cases, so that all scattering effects can be considered purely elastic, and can therefore be treated as a pure wave-interference effect.

For the technique to work, a beam of parallel 'light' is shone upon a sample. Small contrasting features cause a fraction of the light to deviate from its path, thus scattering. This scattered light is then collected on a position-sensitive detector.

As mentioned, scattering occurs when contrasting features are present. This has implications to the type of samples that can be measured. Among the samples that can be analyzed with small-angle scattering are proteins in solution, polydisperse particles, pore structures and density differences in single-phase samples. What is important is that there is a contrast between the particle or pore, and the surrounding material in the sample. The type of contrast varies depending on the type of radiation used. In small-angle x-ray scattering this is

an electron density contrast, for small-angle neutron scattering this is a contrast in neutron scattering cross-section, and for small-angle light scattering this is a transmittance contrast. This difference in contrast type means that if there is a contrast problem while measuring a sample with one technique (i.e. too little or too much contrast), by switching to a different radiation type you may be able to solve your problems.

Like its sister technique, diffraction, small-angle scattering characterizes lengths in a sample. Simply said, small objects scatter a little to larger angles, and large objects scatter a lot to small angles. Since the scattering behavior is highly dependent on the lengths in the sample, some size information can (in most cases) be retrieved. As indicated, the scattering power of an object is highly correlated to its volume. Indeed, the scattering power scales with the volume squared, leading to a dominance of scattering from large objects in polydisperse systems.

A variety of analysis methods can be used to interpret the scattering behavior. These analysis methods revolve around a mathematical construct known as the Fourier transform. Effectively, the observed scattering can be calculated as the Fourier transform of the real-space structure. In other words, a measurement is a physical Fourier transform of your sample. Unfortunately, most detectors can only measure the intensity of the Fourier transform, and not its complementary phase information, and thus vital information is lost which complicates data interpretation.

A marked difference from diffraction techniques is that the small-angle scattering pattern does not contain much information. Indeed, without information on the sample morphology obtained from other techniques such as microscopy, the small-angle scattering information is open to a multitude of interpretations (technically, this is true of diffraction as well, but methods have been developed to get around this problem for some diffraction data). So why would we choose to use this technique as opposed to, say, microscopic methods?

1.2.3 Comparison with microscopy techniques

Microscopy methods are the first techniques that come to mind when faced with a problem involving the analysis of small particles, and for good reasons. Microscopy allows for visualization of objects of virtually any size below a centimeter or so. Optical and confocal microscopes can image objects to sub-micron resolution. Scanning electron microscopes image down to several hundred nanometers, and transmission electron microscopes go even further

down, sometimes to near-atomic resolution. Scanning-probe microscopes can probe along the entire size-range. (For sizes comparable to those probed by small-angle scattering techniques, optical microscopy is often not an option and will not be considered beyond this point.)

But if you talk to microscopists, you will find that one of the bigger challenges in the successful application of microscopy lies in the sample preparation. The further down you want to go in size, the more complex the preparation can become, and many (soft) samples can therefore not be measured properly. The sample preparation method may also induce a structure in the sample, for example due to stresses imposed during cutting, grinding or polishing. This can make it difficult to distinguish the sample structure from the induced artifacts.

But even if the sample preparation is done perfectly, you can only observe a small fraction of the complete sample at a time. In order to get a good statistical average, you need to prepare many samples and measure each sample at multiple locations. This is far from impossible, but it makes you start to wonder if there would be another solution to your problem.

Finally, if you are interested in observing your sample in-vivo or in-situ, e.g. under reaction conditions or high pressure, microscopic techniques often fail to offer solutions.

With small-angle scattering, these problems are substituted for others (which we will come to in a minute). Firstly, small-angle scattering requires only very little, if any, sample preparation. Liquid samples can be measured in capillaries, for example, and fibre samples can be measured simply by suspending the fibre in the beam. Many in-situ reactors can also be used so that reactions can be probed as they proceed.

An additional benefit is that the information present in the scattering pattern pertains to all objects in the irradiated volume. This means that if you want to get an average particles parameter over billions of particles in a suspension, all you need to do is make sure the irradiated sample volume is large enough to contain a billion particles. In small-angle x-ray scattering, volumes of about one to several cubic millimeters are commonly probed. For neutron scattering techniques, this irradiated volume is usually a cubic centimeter or more!

So there are certainly advantages of using small-angle scattering methods over microscopes methods, yet microscopes dominate laboratories. The reasons are partially related to the challenges of analysis of small-angle scattering patterns, and the challenges of collecting a good scattering pattern.

1.2.4 Challenges with small angle x-ray scattering

There are many fine details about the challenges of SAXS. Besides the challenges of collecting a near-perfect scattering pattern (which in many cases can be overcome through hard work and understanding), the main issue lies with the data analysis.

If you have managed to collect the perfect background-subtracted scattering pattern (in the right angular region, on an absolute scale, with uncertainties for each data point, corrected for detector imperfections, and so on and so forth, which we will get to in the next section), the road ahead may still be unclear. The problem lies mainly in the ambiguity of the data, which has become ambiguous since we have lost information in the scattering process (as we have detected only the scattering intensity and have lost the phase information of the Fourier transform). The most clear example of this loss is that particle shape and polydispersity can no longer both be retrieved.

This is another important concept in scattering; you can only determine the polydispersity if you know the particle shape, and you can only determine the particle shape if you have information on the polydispersity (for example if you have a monodisperse sample of proteins in solution, or if you have information on the distribution shape). This means experimentally that, in order to get convincing results of your SAXS data analysis, you need complementary microscopy information. Even with all the information, data fitting still often remains a time-consuming task.

In short then, the technique is still (a hundred years after conception) in dire need of development, mostly in terms of data analysis. The approach provided in this document will get you part of the way towards an answer. The `lookingatnothing.com` weblog aims to collect some of the information on the web for other users and developers, and adding a bit more of my own research, in the hope that we can get closer to making small-angle scattering easy.

More details on scattering can be found in Appendix .1.

Chapter 2

Collecting the perfect scattering pattern

2.1 Corrections

2.1.1 What corrections?

A SAXS measurement is never just a SAXS measurement. In order to get something useful out of SAXS, there are some corrections to make to the data before it starts talking sense. For the perfect SAXS measurement, there are quite a few more corrections one could consider to do. This section explains a few details about some corrections that can be considered to improve the data quality. The information provided here is not strictly necessary for collecting good data but provides a bit of background to illustrate the necessity for some corrections.

2.1.2 Detector corrections

Introduction to detector corrections

In order to detect x-rays, a wide variety of detectors have become available. Depending on the detection method, imperfections and physical limitations may cause a deviation of the detected signal from the true signal (the number of scattered photons). In a perfect case, you would measure the same (true) scattering signal irrespective of the type of detector used.

Real detectors, however, have imperfections, tradeoffs and drawbacks. Some of these detectors and their individual drawbacks will be discussed here, but first, a list of possible distortions will be listed. The distortions can be divided into two categories, intensity distortions and geometry distortions. Intensity distortions are deviations in the *amount* of measured intensity, and geometry distortions are deviations in the *location* of the detected intensity.

Intensity distortions

Intensity distortions are differences between measured intensity and incoming intensity.

The most common distortion (if it can be called that) is that many detectors measure on a relative (but proportional) scale instead of counting the photons. In other words, these detectors measure a certain intensity value in one pixel, and a lower (or higher) intensity value in another. The relative difference between these two intensities are proportional to the difference in number of photons detected, but do not give the number of photons that have been detected. This also has implications later on for the determination of the error in the data. This can be corrected for by measuring a sample of which the absolute response is known, which will be referred to as the absolute intensity calibration.

The second most common distortion is a limited intensity window within which the intensity measured is proportional (in case of relative intensity detection) or equal (in the case of photon detection) to the number of incoming photons. All detectors have an upper detection limit, above which the detector no longer accurately reflects the intensity or the number of photons. Some detectors (in particular non-photon counting, relative intensity detectors) also have a lower limit or noise limit below which the detected intensity no longer is proportional to the incoming photons. Knowing which detected intensity levels are reliable and which fall outside of the linear response region (dynamic range) of the detector is important to the correct evaluation of the data. A correction curve (gamma correction) may in some cases be used to compensate for this, but it is safer to measure intensities within the linear detector response region.

Then there are intensity distortions related to detector electronic noise (again, mostly for relative intensity detection systems) or read-out noise. These consist of the addition of a mostly constant background (noise floor). This is compensated for with a "darkcurrent" measurement, i.e. a measurement of the detector signal without any incoming X-Rays is used to compensate for this. This darkcurrent may have a time-dependent and non-time dependent contribution, so

the darkcurrent measurement duration should approach that of the real measurement [Barna *et al.*, 1999].

Subsequently there may be amplification distortions in these detectors where the amplification for one pixel (or a set of pixels) is different than the amplification for another pixel or pixel set. This may happen when different electronic amplifiers are used for different segments in detectors, due to optical attenuation of certain pixels as a result of manufacturing imperfections, dead pixels, vignetting effects, and so on and so forth. The correction for this is to measure a "flatfield" image: an image of the (per-pixel) detector response for a constant (flat) radiation field.

Amplification drift is one of the more difficult distortions to correct for. This is a gradual drift in amplification factor in time for the electronic amplifiers used. A similar effect happens in imageplates, where due to spontaneous emission, the detected intensity on the imageplate is not stable over time. While in imageplates the time-dependence of the detected intensity versus the true (original) intensity is well-understood and can be compensated for, the only way to deal with electronic amplification drift is to recalibrate from time to time and to measure the drift and uncertainty for each detector.

The last distortion is the detection of spurious signals, spikes ("zingers"), external events and the likes. For example, cosmic rays may cause a "streak" of intensity to be detected, or a detection element may misfire, leading to the detection of a large amount of intensity localized in a single spot. These are sometimes corrected for by the detector or the detection system itself, but in other cases they are not taken into account. In these cases, it is prudent to take two (or three) measurements during the experiment, and subsequently remove any intensity that appears in one measurement, and does not appear in the other [Barna *et al.*, 1999]. The remaining intensity which is present in both can be added to regain the signal-to-noise ratio similar to what it would have been if only a single measurement were taken.

Geometry distortions

Geometry distortions are differences between the position of the photon in the image and the position the photon landed on the detector surface.

Differences in these positions mostly affects two types of detectors: wire detectors and CCD or CMOS cameras based on a fluorescent screen and an optical guidepath (image intensifiers included). Detectors which should be unaffected by this are imageplates (where it depends on the accuracy of the scanner motor

drives), direct-detection systems such as the PILATUS [Eikenberry *et al.*, 2003] or Hamamatsu flatpanel detectors, and fibreoptics-based CCD and CMOS detectors with a fibreoptic guidepath between fluorescent screen and semiconductor plate.

With wire detectors a peculiar geometry distortion can occur. In these detectors, photons cause an avalanche effect in the gas which fills the wire chamber [Né *et al.*, 1997]. The avalanche frees electrons in the gas which are detected by the wires (incidentally, the avalanche magnitude is proportional to the photon energy, which in turn affects the magnitude of the electrical signal detected. This allows for easy electronic "filtering" of photons which are not of the desired energy, such as cosmic rays). The avalanche center position is detected using the temporal delay of the electric pulse, i.e. the time delay of the arrival of the pulse at one end and the other end of the wire. This method can cause a peculiar type of geometry distortion at elevated levels of incoming photon flux, worsening as the flux increases. This can be easily conceptualized when imagining a second photon striking the detection wire while the pulse of the prior photon is still being detected. This will cause wrong "pairing" of pulses (i.e. the time arrival of a pulse of the first photon at one end of the wire is compared with the time arrival of the pulse of the second photon on the other end of the wire). There is no post-mortem correction of this type of geometry distortion.

Most detectors based on indirect detection (phosphor screen, gas avalanche chamber) often do not detect the photon exactly where it struck, but in a region around this point. Thus, the detected pattern is "blurred", or convoluted with a smearing function. This can be corrected for, but since de-smearing is prone to errors, the safest way to account for this is to smear the model fitting function in a similar fashion as the effects of the smearing on the detector.

Then there are a variety of reasons for a gradual geometry distortion in a variety of detectors. These distortions gradually worsen or improve over the entire detector, and can take the form of pincushion-type distortions or other types. These distortions can be corrected for by placing a mask with a regular pattern before the detector, and measuring the deviations from the regularity of the pattern in the detected image. A distortion map can be made based on this, and detected pixels can be reassigned their true coordinates based on this map.

Lastly there may be pixel-dependent distortions or sharp dislocations due to dislocations in fibre-optics or cracks in real optics. In these cases it is best to consult the manufacturer of the detector to discuss the appropriate course of action.

Which detector suffers from what distortions and to what degree?

This section is for orientational purposes only, and the particular distortions and the severity thereof need to be established for each detector individually.

The direct-detection, photon counting detectors (such as the PILATUS detector from the PSI detector group), where the photon is directly detected onto a semiconductor chip usually suffer from very few distortions, if any. There is no appreciable geometry distortion, little to no electronic noise (background) problems, and little effect from external signals due to energy discrimination. The sensitivity of individual pixels may decrease upon increased exposure, and there may be dead pixels, which should be compensated for with a flatfield correction and a mask, respectively. Some flatpanel detectors may not be photon-sensitive, and therefore also require calibration. Calibration for absolute intensity is a good idea for both detectors to correct for some other aspects as well.

The second type of photon detectors are wire chamber detectors. These suffer from a narrow linear response range, and due care needs to be taken not to exceed said limits. Positioning errors may be severe, depending on the wires used (a high-delay wire will give you accurate positions, but lousy maximum countrates, and vice versa). Some gradual position distortion may also be present, so a distortion map using a patterned mask is to be made. Oxidation on the wires due to overexposure may reduce sensitivity at points on the detector, necessitating a flatfield image. Images will be convoluted with a smearing (point-spread) function.

Imageplate detectors suffer from slow read-out times, but otherwise are quite distortion-free. Most are not photon-sensitive and detect only relative intensities, but over a very wide linear response range. They are sensitive to a wider range of photon energies than the aforementioned detectors and some zingers and spikes may appear. Overexposure may also reduce sensitivity at spots on old imageplates. Geometric distortions should be limited to mechanical inaccuracies in the readout mechanics and should be effectively zero. There is some amplification drift over time, so care must be taken to either correct for this (automatic imageplate detectors with built-in readers should do this), or to wait 20 minutes before measuring an imageplate so that the worst drift has passed. The point-spread function on these detectors is much more limited than for wire detectors.

Then we come to indirect detectors often based on a fluorescent material deposited on a screen, which emits photons in the visible light region when ex-

cited by X-ray photons. This visible light is then optionally amplified using an image amplifier before detection using optical CCD or CMOS detectors. Often, focusing optics or fibreoptics are used to reduce the size of the image on the detection screen to the size of the CCD or CMOS chip. Some systems use multiple, stacked chips to increase the number of detected pixels, where each chip has its own amplifier and readout cirquit. These detectors suffer from almost all of the distortions mentioned in the previous paragraph [Barna *et al.*, 1999]. They may show zingers and cosmic rays, different background and amplification drift per chip, mild to severe geometric distortions (especially when image amplifiers are used), some vignetting (optical systems), different detection efficiencies per pixel, each of which may vary over time. A regular check between the response of this detector and that of an imageplate or direct-detection detector should give clear clues as to which distortions need correcting for.

How much does it really matter?

This is the question which should be foremost in your mind at this point. And the answer is that it matters, especially when there are no significant features in a small-angle scattering pattern such as peaks or bumps, and a monotonously decreasing intensity is all that is available. In such systems, a change in slope due to vignetting, combined with non-linear behaviour around the beamstop will ruin any chance of successful analysis. The danger is that the analysis method (curve fitting to one or the other model) will likely still succeed in giving you a good agreement between fit and data, with some reasonable morphological parameters resulting. However, the morphological parameters will not correspond well with the real structure in the sample.

This could be a good reason, therefore, to explain why many measurement (and analysis) results vary from beamline to beamline. From literature, it is made clear that the application of some of these corrections can bring the detected intensity accuracy to 1-2% without too much trouble (for CCD detectors), and to sub-percent levels with more effort [Barna *et al.*, 1999]. Preparation of a calibration sample (f.ex. calibrated glassy carbon) which can be measured at each beamline should give more insight into the variance between the detector responses. Efforts are underway to compare a small set of detectors at SPring-8 to identify the main distortions of some of the detectors. This document will be updated when that becomes available.

2.1.3 Transmission, time and thickness corrections

Since many samples absorb a small fraction of radiation, this fraction does not contribute to the scattering effect. Therefore, the degree of absorption of a particular energy of radiation needs to be determined for each sample, and this needs to be corrected for. There are a few ways of measuring the transmission factor.

One way to measure the transmission factor of a sample is to measure the beam flux of the x-ray beam before and after the sample has been inserted. This can be done by some detectors after attenuation of the primary beam (to avoid damaging the detector), by means of a beamstop-mounted photodiode, or by insertion of a strongly scattering material behind the sample position. In the first two cases, the ratio of the two fluxes (before and after insertion of the sample) is the transmission factor. In the second case, the ratio of the two *integrated* intensities on the detector is the transmission factor:

$$T = \frac{I_1}{I_0} \tag{2.1}$$

where T is the transmission (ranging from 0 to 1), I_0 is the intensity of the primary beam without sample, and I_1 the intensity of the beam after insertion (and downstream) of the sample.

An alternative way of measuring this is to place a special kind of x-ray detector called an "ionisztion chamber" before (upstream) and behind (downstream of) the sample. The transmission factor is determined by the ratio of the ratio of the two ion chambers before and after insertion of the sample. The advantage of this (and of the beamstop-mounted pin-diode) is that online transmission measurements are now possible. In other words, you can determine the transmission factor at any moment during the measurement, which allows checking for (some cases of) sample degradation or movement. A second advantage is that with this method, variations in primary beam intensity are compensated for. The disadvantage is that the ion chambers only work in the presence of some gas (usually air), and can therefore only be used with SAXS machines with an open-air sample position (or come at the expense of additional background scattering as a ion-chamber gas environment has to be built). The equation for this is:

$$T = \frac{\frac{I_{d,1}}{I_{u,1}}}{\frac{I_{d,0}}{I_{u,0}}} = \frac{I_{d,1} I_{u,0}}{I_{u,1} I_{d,0}} \tag{2.2}$$

where T is the transmission factor (ranging from 0 to 1), the subscript $_d$ indicates the downstream ion chamber, $_u$ indicates the upstream ion chamber, and as in

the previous example, the subscript $_0$ indicates before sample insertion, and $_1$ after sample insertion. Sample in this case means sample plus capillary and solvent.

The second correction, time correction is a straightforward one. The longer the measurement, the more intensity is detected. This is corrected for by simple division of the measured intensity with the measurement time.

Lastly, the thicker the sample, the more scattering material is in the beam. While this is often related to the transmission factor correction, it is not the same, and needs to be corrected for separately by normalizing to the thickness of the sample.

2.1.4 Absolute intensity correction

A large number of detector- and geometry-specific variables can be corrected for by performing an "absolute intensity calibration". This is excellently explained by Dreiss *et al.* [2006] (whose method we follow here). In short, we are calibrating the intensity through the use of a calibration sample. The scattering of this sample in absolute intensity units is known beforehand, and a calibrated datafile should come with the sample (in the case of scattering from so-called "primary calibration samples" such as water, the scattering in absolute units can be easily calculated)[WIGNALL and BATES, 1987; Zhang *et al.*, 2010]. By comparing the intensity in the calibrated datafile with the intensity as determined on the SAXS machine you use, a calibration factor CF can be determined. This is done (with the necessary corrections) through:

$$CF = \left(\frac{\delta\Sigma}{\delta\Omega}\right)_{st}(q)\frac{d_{st}T_{st}}{I_{st\Omega}} \tag{2.3}$$

where the subscript $_{st}$ denotes the calibration standard, T is the transmission factor, d is the thickness of the sample, and I is the measured intensity (after application of the detector and background corrections) and $\left(\frac{\delta\Sigma}{\delta\Omega}\right)_{st}(q)$ is the known scattering pattern (calibrated datafile) from the calibration sample. The calibration factor can be determined by a least-squares fit or linear regression (least squares allows for inclusion of counting statistics).

2.1.5 Background correction

Everything scatters, even if only a tiny bit. Most SAXS instruments do not have an uninterrupted vacuum flightpath, and have x-ray transparent separation windows between the vacuum and the outisde atmosphere (or detector gas), and these windows scatter slightly (with the exception of single-crystalline materials such as (CVD) diamond or sapphire). Air also scatters, as do solvents, capillaries and so on and so forth. This results in a certain amount of background scattering which adds to your detected signal. Since this scattering is not always uniform (it usually isn't), it has to be corrected for to prevent misanalysis of the data.

The background measurement consists of a measurement exactly like the sample measurement, minus the sample. In liquid systems, this means a measurement of a capillary with just the solvent (ideally the exact same capillary used for the sample measurement). Since the uncertainties of the intensity (we will come back to this later) of the background measurement is *added* to that of the original measurement, measuring the background for a longer time than the sample may be advantageous (especially if many samples are measured which can use the same background measurement). In the correction procedure, we compensate for the transmission, thickness and measurement time of the background separately, so that even if they are different, they do not affect the resulting data.

2.1.6 Correcting for spherical angles

Most detectors are flat with uniform, square pixels, but we wish to collect the intensity over a solid angle of a (virtual) sphere. The projection of the detector pixels on the sphere results in a difference in solid angle covered by each pixel (illustrated in Figure 2.1). Therefore, we need to correct the intensity for the difference between these areas. This is further exacerbated if the detector is tilted with respect to the beam (and thus has a "point of normal incidence" from the sample which differs from the direct beam position). This sounds complicated but is achieved by means of a few geometrical parameters. This correction is given by [Boesecke and Diat, 1997] as:

$$\frac{L_P^2}{p_x p_y}\frac{L_P}{L_0} \tag{2.4}$$

where L_P is the distance from the sample to the pixel, L_0 the distance from the sample to the point of normal incidence (abbreviated as *poni*, usually identical

to the direct beam position except in case of tilted detectors), and p_x and p_y are the sizes of the pixels in the horizontal and vertical direction, respectively.

2.1.7 Putting it all together

The measured intensities should be corrected to spherical angles, for the dark-current intensity and for the pixel quantum efficiency (leaving aside geometric corrections for the time being), described by [Boesecke and Diat, 1997]:

$$I_\Omega = (1/i_0)\frac{I_d/t_d - I_{dc}/t_{dc}}{I_{qe}}\frac{L_P^2}{p_x p_y}\frac{L_P}{L_0} \tag{2.5}$$

where i_0 the incoming flux for the sample measurement, I_d the raw detector pixels, t_d the time of the measurement, I_{dc} the darkcurrent measurement, t_{dc} the darkcurrent measurement time (ideally approaching the measurement time as it may have a time-dependent component and a constant addition), I_{qe} the optional quantum efficiency of the detector (from flatfield image), L_P the distance from the sample to the pixel, L_0 the distance from the sample to the point of normal incidence (abbreviated as poni, usually identical to the direct beam position except in case of tilted detectors), and p_x and p_y are the sizes of the pixels in the horizontal and vertical direction, respectively.

At this point, I_Ω can be binned (also called "integration" for isotropically scattering samples) to drastically reduce the data size and reduce the statistical errors on the data. For anisotropically scattering samples, this binning should not be done.

Then, I_Ω should be corrected for the background measurement (denoted with the subscript $_b$), the transmission factor and the sample thickness:

$$I_c = \frac{I_{s\Omega}}{d_s T_s} - \frac{I_{b\Omega}}{d_b T_b} \tag{2.6}$$

And finally, the intensity should be set to absolute units:

$$\left(\frac{\delta\Sigma}{\delta\Omega}\right)_s (q) = \mathrm{CF} I_c \tag{2.7}$$

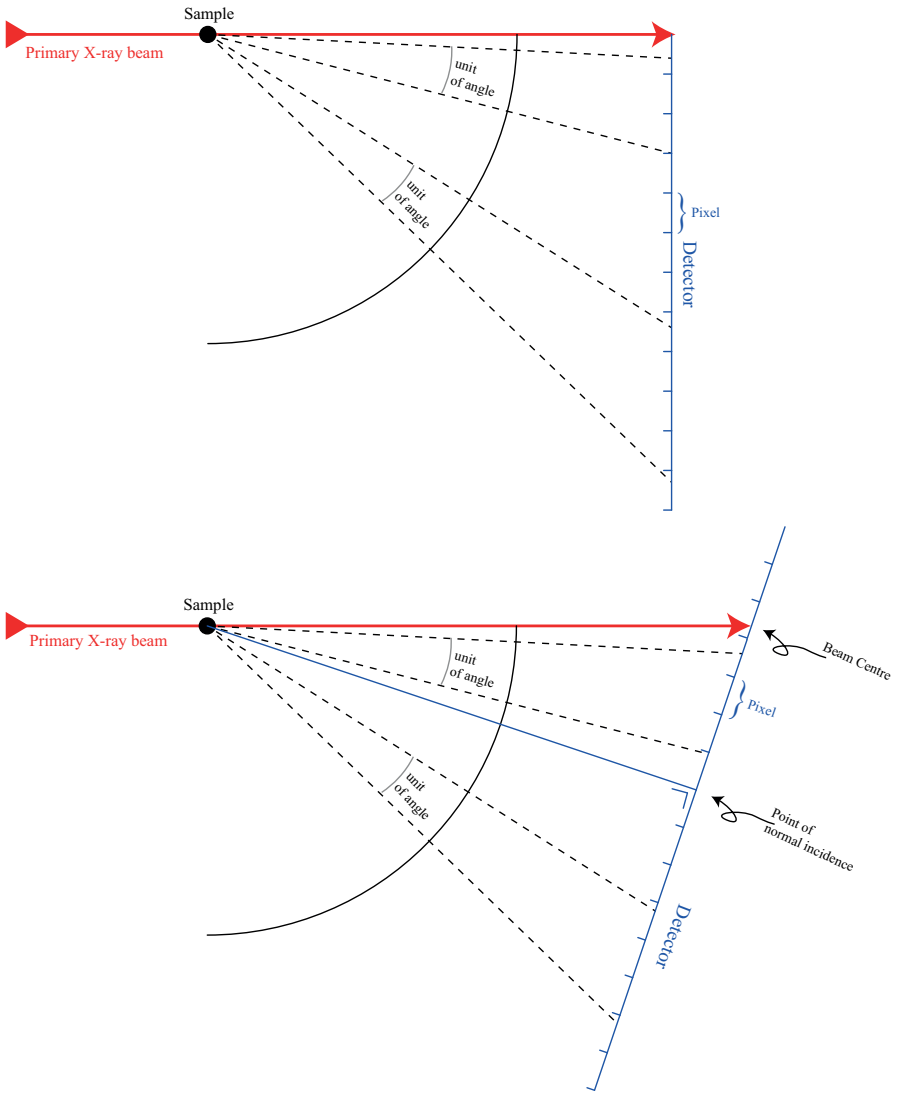

Figure 2.1: *The need for spherical corrections illustrated for straight (top) and tilted (bottom) detectors. One unit angle covers a different number of pixels depending on angle in both cases, which needs to be corrected for.*

2.2 How to perform the perfect measurement

2.2.1 Things you need to know

Before starting this section, there are a few things you should know. The first is the definition of the scattering angle q. While diffractionists have no qualms about defining their diffraction angles in degrees "two theta", small-angle scattering data reduction often involves making these angles independent of the wavelength. For a variety of reasons (some of which will become clear later on), the small-angle scattering angle is usually defined as:

$$q = \frac{4\pi \sin(\theta)}{\lambda} \tag{2.8}$$

where θ is half of the scattering angle (in accordance with diffraction, the full scattering angle is defined as 2θ), and λ is the wavelength of the radiation used. The units of the scattering vector q are then in reciprocal length-units. If the wavelength is entered in Ångström, q has the units of $Å^{-1}$, and if λ is given in meters, q assumes the units of m^{-1}. Bear in mind that when moving in q-space from one unit to the other, one moves with the inverse of the scaling factor, i.e. $q = 1\text{nm}^{-}1 = 1 \times 10^{9}\text{m}$ (while many experimentalists work with q in inverse nanometers or inverse Ångström, I will attempt to use only inverse meters in this document for its universality). In literature, one can find some other definitions of scattering vector, but most are very similar to the one used here.

2.2.2 Before you begin

Before you begin any SAXS experiment, there are a few questions which you should be able to answer:

1. What is the ballpark region of the size of the objects to characterize
2. How many phases are there in the sample? (i.e. contrasting phases, such as polymer and water (2), metal and vacuum (2), block copolymer component A and B (2), etc.)
3. What is the contrast between the phases in the sample?
4. What volume fraction do the objects take up?
5. Is the sample radiation sensitive?

6. What analysis method will be applied?
7. What wavelength will be used or what would be preferred?
8. How are you planning to store, log and backup your measurements and the measurement details?

Each question has an underlying reason; each of which will be discussed.

A general idea about the size of the objects you want to measure is necessary to determine which (small) angles to measure. Unfortunately, most SAXS equipment can only collect a limited angular region, maybe one or two decades in q are collected sufficiently well. Therefore, one must be able to supply a ballpark size radius R, which can then be converted to a value in q-space by:

$$q_{\Delta} = \frac{pi}{R} \tag{2.9}$$

This value q_{Δ} signifies the periodicity of the oscillations in the scattering pattern of spherical particles of that size. A simulated scattering pattern of monodisperse 10nm spheres is shown in Figure 2.2 in semi- and double-logarithmic graphs. The periodicity of the oscillations is $q_{\Delta} = \frac{pi}{1\times10^{-8}}$. It is good practice in SAXS measurements to measure in a range with this value in its logarithmic center, i.e. if two decades of q can be measured, ensure that the range of $\pi \times 10^7 \leq q \leq \pi \times 10^9$ can be accurately measured. As shown in figure 2.2, this will measure both the initial region as well as the final power-law decay slope most signals revert to at higher angles. For polydisperse samples, the choice of ballpark size radius should be heavily skewed to the sizes of the larger objects one wants to observe.

The number of phases and their contrast in the sample is important, in order to determine the probability of success of the measurement and its analysis. Most samples with two contrasting phases will not pose many problems in the analysis. However, when the number of phases is increased, the analysis becomes magnitudes more complex as all contrasts between all phases have to be considered. For a three-phase sample, i.e. water, polymer and vacuum in a partially immersed porous polymer, the contrasts between the water-phase and polymer phase, water-phase and vacuum phase, and polymer and vacuum must be considered. Since the scattering power is proportional to the square of the electron density contrast, if the difference between the water-phase and the polymer phase is small (i.e. when analyzing a polymer with a density of 1.1 g/cm^3), the water-phase and polymer phase can be considered to be a single phase contrasting with vacuum.

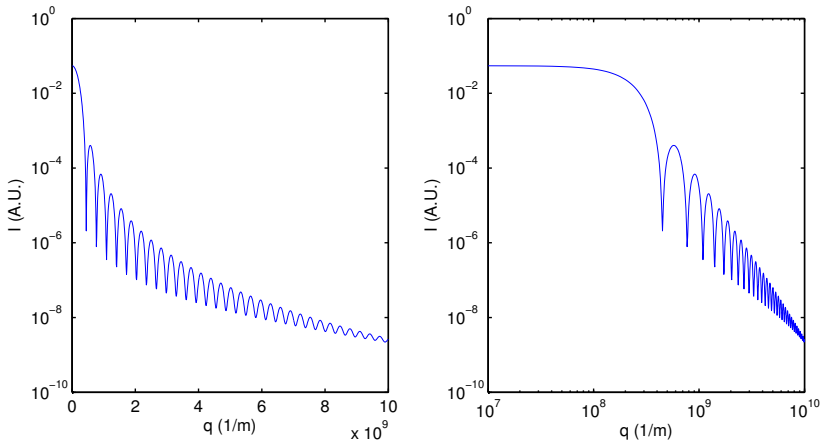

Figure 2.2: *Simulated scattering from a sphere 10 nm in radius.*

The volume fraction of scatterers matters, because scatterers in close proximity scatter differently than dilute scatterers for a variety of reasons. Whenever possible, each sample should be measured at a few different concentrations, to ensure that concentration effects do not affect the scattering. Volume fractions of one to a few percent should be sufficiently low as a rule-of-thumb, but it never hurts to check. A large volume fraction of scatterers (i.e. more than 10%) will necessitate analysis with more advanced, restrictive and complicated analysis models, greatly adding to the complexity of the endeavor.

If the sample is radiation sensitive, as most things are to some extent, one has to consider the duration of the experiment and checks for the effects of radiation damage on the scattering pattern. This can be addressed by taking multiple measurements of the same (static) sample to identify exposure-dependent changes, and performing these measurements for multiple samples. Measuring 5 or more samples of the same material will as an added bonus result in an estimate for the statistical uncertainties of the physical parameters determined through data fitting. The measurement of these duplicates must be considered in the beamtime time-planning.

The choice of analysis method affects the quality and range in which the data needs to be collected. Analysis methods focusing on the tailing behavior of the scattering (and thus the smaller surface- and interface-specific details) require measurements to higher q, and conversely, methods (such as the Guinier method) focusing on the initial scattering behaviour (i.e. before the first "dip" in Figure 2.2) require a shift to lower q. As mentioned, the scattering from polydisperse systems is heavily skewed to express contributions from large scatterers (as the scattering power of a particle is proportional to the square of the volume)

and thus also need a shift to lower q. Additionally, for more complex analysis models such as inverse Fourier transforms or Monte-Carlo fitting, a large number of detected photons are required to improve the statistics of the detected signal sufficiently. For such models, counting until the extrapolated number of photons at $q = 0$ approaches 10^7 counts may be required (note, however, that many photon-counting detectors do not go this high in their counting electronics, so multiple measurements may be required).

The question of wavelength is a difficult one to find a good answer to, as the wavelength affects many aspects of the experiment. A lower wavelength (higher energy) has a higher penetration depth through samples, but the detector efficiency is generally lower for these. Additionally, choosing a lower wavelength increases the required sample-to-detector distance and reduces the tolerances of the collimation (requiring a longer collimation, resulting in a more parallel beam at the cost of an increased photon loss). Increasing the wavelength (reducing the energy) may result in a large amount of absorption of the radiation by the sample (which should, as a rule-of-thumb, be less than 30%). To arrive at a conclusion, one can first enquire as to what wavelengths are available at the experimental station, and what the photon flux and detector efficiency is at each wavelength. Then the geometrical constraints should be considered, and the sample absorption should be calculated. With all this information a good compromise may be found.

Finally, a word on safeguarding your efforts. It is no use to do four days of measurements only to lose the logbook, forgetting to measure or note down essential information, or being stuck with a broken external hard-drive upon the return to the office. Make sure that there is a solid plan in place to transport the data and a backup of the data, and that there is a well-kept logbook and a back-up (copy or scan) of the relevant pages of the logbook. Make sure that the back-ups travel separately from the other data. In order to ensure completeness of the data, a checklist can be made before the experiment.

2.2.3 Have the beamline staff measure the following

For the reduction and correction algorithms, one has to make sure that the following is known:

The geometric information:

1. ☐ The sample-to-detector distance in meters
2. ☐ The wavelength (in meters). If the photon energy E is supplied in

units of keV, this can be converted to Ångström (1 Å$= 10^{-10}$ m) through $\lambda(\mathring{A}) = 12.398/E(keV)$ (conversion factor from the 2002 NIST CODATA database)

3. ☐ The position of the direct beam on the detector (in pixels)
4. ☐ The point-of-normal-incidence in pixels for tilted detectors (i.e. not mounted perpendicular to the direct beam)

The detector information:

1. ☐ The detector name
2. ☐ The number of pixels in the horizontal and vertical directions
3. ☐ The size of the individual detector pixels in horizontal and vertical directions (in meters)
4. ☐ The detector file data type (f.ex. 'uint16' for 16-bit unsigned integers)
5. ☐ The detector file endianness
6. ☐ The required image transformation to transform the detector output image to the laboratory frame of reference
7. ☐ The detector rotation offset in case of a detector rotated with an arbitrary number of degrees

The correction information:

1. ☐ The filename of the mask image with the masked pixels either set to 0 or maximum intensity (or both), which may be a .png image edited in any image editor
2. ☐ The mask acceptance window for valid pixels (analog to a bandpass filter with a low intensity cut-off and a high-intensity cut-off)
3. ☐ The flatfield image filename (if applicable)
4. ☐ The darkcurrent image filename (if applicable)
5. ☐ The darkcurrent image measurement time (should be identical or close to the measurement duration)
6. ☐ The distortion map filename (if applicable)
7. ☐ The absolute intensity standard sample name
8. ☐ The absolute intensity calibration factor

Also write down information on the collimation geometry for publication and cross-check of q limits. Note the ion chamber and pin-diode amplifier settings (and readings for a "normal" measurement) for troubleshooting ease and transmission calculation. Also ask for motor movement limits and positioning accuracy. Lastly, write down anything that appears to be valuable information (this naturally includes *everything* your beamline manager tells you).

Finally, check if all of the beamline computers are set to the same time and date, and that this is correct.

2.2.4 The user should measure the following

Transmission measurement

For each measurement (indeed, each datafile), the average transmission factor for the duration of the measurement has to be calculated (e.g. for correct background subtraction). The methods for this have been given before. The on-line measurement techniques allow for constant collection of the transmission factor during the measurement (often with a frequency of several Hertz), which should also be stored. Deviations in the transmission factor during the measurement are a good indication of sample instability or motion.

Background measurement

Each sample has a background, consisting of every component except the objects you are trying to characterize. For proteins, this background consists of the solvent and the capillary, for particles in solution equally so, for fibres in air the background consists of the air itself (although fibres should be measured in vacuum whenever possible), and so on and so forth. The quality of the resulting data is also linearly affected by the statistics of the background measurement, so make sure to measure this sufficiently long (at least as long as the normal sample measurement).

Repeat the background measurement for each change in geometrical configuration or change of solvent or capillary type and size.

Sample measurement

The actual sample measurement should be measured long enough for collection of sufficiently accurate intensities, and should be measured multiple times in sequence to check for sample instability (and possible de-zingering although this should already have been done as a low-level correction in the detector electronics itself). Multiple samples of the same material should be measured to determine the statistical uncertainty of the resulting parameters. For dynamic systems this is not always possible, but repeated runs of the same dynamic system should provide some information on uncertainties.

Darkcurrent measurement

Measure a new darkcurrent image (a measurement with the beam shutter closed) in case a CCD or CMOS detector is used, for each measurement duration in your measurement repertoire. Since the darkcurrent images often have a time-dependent and a time-independent component, it is necessary to measure the darkcurrent images for the same time as the actual sample measurement.

in checklist form

The user should determine for each sample:

1. ☐ The sample name (for logging)
2. ☐ The sample filename
3. ☐ The sample measurement duration
4. ☐ The sample transmission factor
5. ☐ The sample thickness (thickness in the direction and location of the direct beam)
6. ☐ The incoming flux onto the sample
7. ☐ Remarkable aspects regarding the sample
8. ☐ The relevant background name (identifier for logging)
9. ☐ The relevant background filename (all information collected for the sample (flux, transmission, etc.) should also be collected for the background measurement)

10. ☐ If necessary, a new darkcurrent measurement should be collected.

Chapter 3

Some final remarks

3.1 Some suggestions for logbook-keeping

Herewith some tips and pointers garnered throughout the beamtimes of the author on how to keep a log-book during the beamtime. In no way should this be seen as the ultimate answer, just as one approach to keeping a log-book.

The logbook is the key to success of your measurements. It contains the information essential to making sense of your thoughts a week, a month or a year after the experiments. The suggested logbook is a paper logbook, with numbered pages. The first page should be kept blank to keep a "table of contents".

All the information you receive at the beginning of your beamtime (wavelength, sample-to-detector distance and so forth) should be written down in the logbook. Pictures taken should be stuck into the logbook with the filename of the pictures written alongside the pictures.

Each sample measurement, calibration measurement, background measurement and so on, should be written down in the logbook with an appropriate time and date before. The filename has to be written down, the measurement duration, the sample description, and any further information.

If the measurement turns out to be remarkable, print out the measured image, and stick it in the logbook (again, writing the filename of the image alongside the image in the logbook). Feel free to draw in the logbook anything of note (changes in temperature, odd sounds, etc.).

Finally (or rather, initially) take a group photo of the group of colleagues who joined the experiment. At the end of the experiment, scan or copy the logbook

and ensure its safety.

3.2 Planning

Depending on the amount of equipment to install, it is generally better to schedule two shorter beamtimes than to do one long experiment. In the time in between the two shorter beamtime, the quality of the collected data can be assessed and improvements can be made to equipment. Additionally, fatigue is a great source of photon wastage (if nothing else), and should be avoided at all costs. Make sure you and your members are well-rested before and during the beamtime to prevent damage of equipment due to concentration failure (eight hours of sleep per beamtime day is not a luxury). A good suggestion is to ensure that dinners are always enjoyed outside of the institute with all members present (a long measurement usually can be scheduled around this time).

The first six to 12 hours of any beamtime are often spent aligning the equipment, setting up any sample environments and measuring the calibration measurements. Make sure to account for this when planning.

Prioritize the samples before the experiment to ensure that the most important samples are measured. Also prioritize the calibration measurements. Leaving the beamtime without a good idea of the beam center (for example) can add a lot of complexity to the data analysis!

3.3 Number of assistants or team members

The number of assistants required at beamtimes (dependent on the nature of the measurements) can be approximated as equal to the number of beamtime days plus one. So for a three-day beamtime, four people are needed, and for a one-day beamtime, only two people will be necessary. The upper limit is bound by the complexity of the measurements.

Make sure that all team members are familiar with the technique and the equipment operation.

3.4 Luck

Good luck!

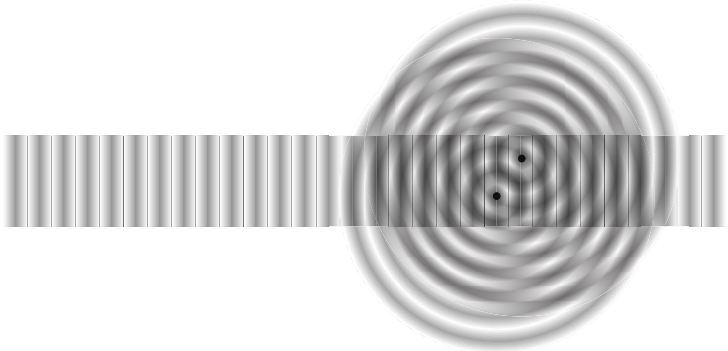

Figure 1: *Two electrons oscillating with an incoming EM wave and emitting interfering waves themselves.*

.1 Detailed aspects of scattering to consider

.1.1 The detail for more complete understanding

Some aspects of small-angle scattering will be focused on here for those willing to dig deeper into the details. Doing so will improve understanding of the technique, and with understanding comes an increased chance of successful completion of your scattering experiment.

.1.2 The basics of scattering

The basis of most scattering techniques based on EM radiation, such as crystallographic techniques, lies in the interaction of incoming radiation with the sample. Imagine two electrons being irradiated by an incoming electromagnetic wave, consisting of an electric and a magnetic field. The electrons respond to the electric field (due to their charge) and will oscillate with the same frequency as the field supplied by the incoming wave [*]*. When the two electrons oscillate, they emit radiation at the same frequency as their oscillation. If these two electrons are situated in close proximity, this radiation can interfere (c.f. Figure 1). When the emitted radiation is observed from a distance, the interference causes the appearance of maxima and minima in the detected intensity of the radiation.*

[*]the electrons usually oscillate with the same, or virtually the same frequency (also known as "elastic" interaction with the incoming radiation). There are, of course, exceptions to this ("inelastic" interactions, mentioned in a previous footnote) which can be exploited, but they go beyond the scope of this document and have therefore been omitted.

Practical scattering experiments differ from this idealised situation in several aspects, but the essence remains valid. The differences are that in practice:

- The incoming wave is replaced by a superposition of waves that are roughly in phase within a certain volume of space
- The experimental sample consists of many electrons instead of just two
- The detector cannot observe the scattering amplitude (and thus cannot resolve the phase of the scattered radiation), but instead detects the scattering intensity (photon flux) striking the detector surface. Further instrumental limitations also affect the observed intensity pattern.

These three aspects will be discussed in detail in the following paragraphs, with special emphasis on the second and the third aspect, as they are of specific relevance to most measurements.

Some useful equations related to the behaviour of waves

Since photons can be considered to have a particle as well as a wave nature, they can be described using either. The de Broglie relationships link the kinetic energy E, momentum p, wavelength λ and frequency ν. Since radiation can be described by any of these, it is useful to keep the following equations at hand:

$$\lambda = \frac{h}{p} \tag{1}$$

Here, h is the Planck constant. Similar equations can be established for an electromagnetic wave linking the angular wavenumber k, angular frequency ω, frequency ν and energy E:

$$k = \frac{2\pi}{\lambda} = \frac{2\pi\nu}{v_p} = \frac{\omega}{v_p} = \frac{E}{\bar{h}c} \tag{2}$$

where v_p is the propagation speed of the wave and equal to c for waves travelling in vacuum, and $\bar{h} = \frac{h}{2\pi}$ is the reduced Planck constant. The value for the Planck constant is $6.626 \times 10^{-34}\mathrm{Js} = 4.136 \times 10^{-15}\mathrm{eVs}$.

The electric field amplitude of an electric field propagating along the x-axis, can be expressed as a sine wave in its real form $E_0 \sin(kx)$ or in its complex form $E_0 \exp i(kx)$, where $k = \frac{2\pi}{\lambda}$ is the wavenumber. The electric field of EM

radiation can be parameterized in vector notation using a single equation [Als-Nielsen and McMorrow, 2004]:

$$\mathbf{E}(\mathbf{r},t) = \hat{\epsilon}E_0 \exp i(\mathbf{k}\cdot\mathbf{r} - \omega t) \tag{3}$$

where $\hat{\epsilon}$ is the polarisation vector (the direction of the oscillatory field), t is the temporal component, $\mathbf{k}$ the wavevector along the direction of propagation.

The intensity of radiation emitted by an electron oscillating in an electric field is related to the intensity of the incoming radiation by the Thompson equation:

$$I_e(\theta) = I_p\frac{T}{R^2} = I_p\frac{\frac{e^4}{m^2c^4}P}{R^2} \tag{4}$$

Where I_p is the intensity of the incoming radiation, T the product of the square of the so-called classical electron radius ($r_e^2 = \frac{e^4}{m^2c^4} \approx 7.90e-26$, e is electron charge, m electron mass and c the speed of light) with the angle-dependent polarisation factor P. R denotes the distance between the electron and the "detector".

The polarisation factor is dependent on the source of the X-rays, and direction of observation. For synchrotron radiation, the incoming radiation is polarised in the horizontal plane, making the polarisation factor for observations in the vertical plane equal to 1, and for observations in the horizontal plane equal to $P = \cos^2(2\theta)$, where 2θ the scattering angle. For unpolarised sources, $P = \frac{1+cos^2(2\theta)}{2}$. When small angles are considered, the polarisation factor in all cases can be approximated to 1.

To calculate the position of constructive and destructive interference for two point scatterers, it can be shown that this is dependent on the relative locations in 3D space of the two scattering centers, using two special, easy to calculate cases (not shown here). We can then consider the more complex case of two arbitrarily positioned point scatterers, as shown in Figure 2. We see here that the difference in pathlength is the sum of ΔLa and ΔLb. These can be written as the projection of $\mathbf{r}$ onto $\mathbf{k}_i$ and $\mathbf{k}_o$ respectively, where $\mid \mathbf{k} \mid = \frac{2\pi}{\lambda}$:

$$\begin{aligned} \Delta La &= \mathbf{r}\cdot\mathbf{k}_i \\ \Delta Lb &= \mathbf{r}\cdot\mathbf{k}_o \\ \Delta L &= \Delta La + \Delta Lb \\ &= \mathbf{r}\cdot(\mathbf{k}_o - \mathbf{k}_i) \\ &= \mathbf{r}\cdot\mathbf{q} \end{aligned} \tag{5}$$

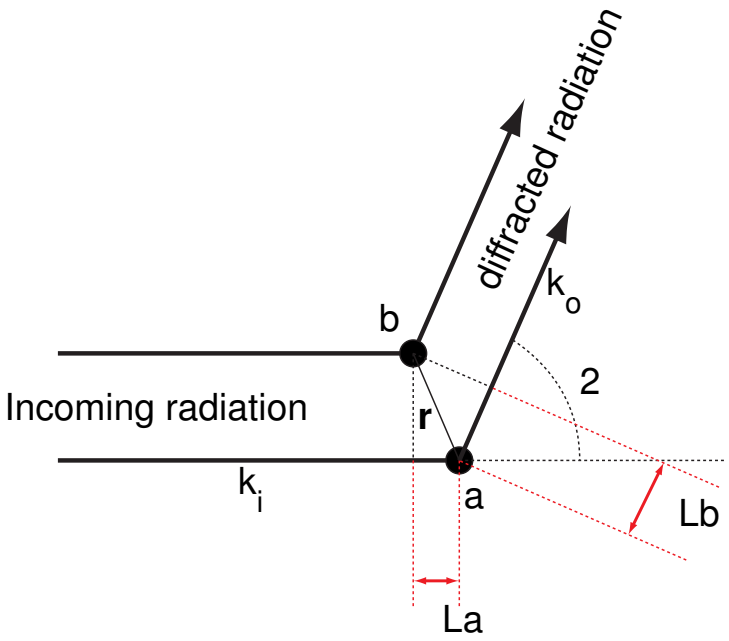

Figure 2: *Two electrons positioned arbitrarily with respect to the incoming radiation, oscillating with an incoming EM wave and emitting interfering waves themselves.*

The last part of this equation is our definition of $\mathbf{q}$, defined as:

$$\mathbf{q} = \mathbf{k}_o - \mathbf{k}_i \tag{6}$$

with magnitude

$$q = \mid \mathbf{q} \mid = \mid \mathbf{k}_o - \mathbf{k}_i \mid = \frac{2\pi}{\lambda} 2\sin(\Theta) \tag{7}$$

as shown graphically in (Figure 3). The phase difference caused by this path-length is:

$$\Delta\Phi = \mathbf{q} \cdot \mathbf{r} = 2\sin(\Theta) \mid \mathbf{q} \mid \cdot \mid \mathbf{r} \mid \tag{8}$$

.1.3 Incoming waves - coherence volumes

Only a small fraction of the incoming waves actually interact with the electrons in the sample. This means that performing scattering experiments requires high-flux sources producing high intensity waves. In the visible region of the EM spectrum, lasers are commonly used for two reasons: lasers are a high-flux source, and secondly produce monochromatic radiation (the monochromaticity is important for reasons discussed shortly hereafter). For the X-ray section of

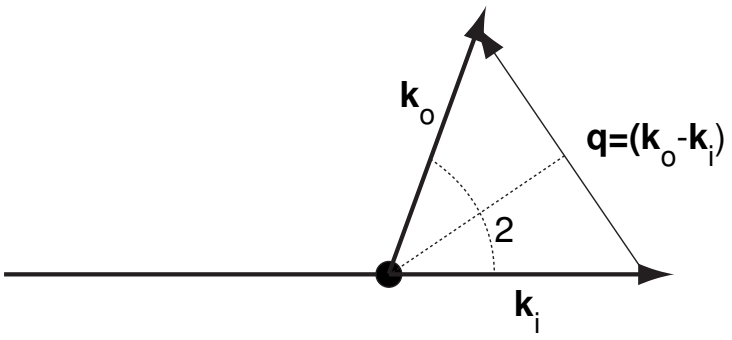

Figure 3: *Definition of* $\mathbf{q}$ *as* $\mathbf{k}_o - \mathbf{k}_i$.

the EM spectrum, a variety of sources are available. Most X-ray sources, however, do not produce monochromatic radiation.

The monochromatic radiation is of importance in scattering experiments, as a local volume at the sample position has to be established, where the waves are in phase. The size of this volume depends partially on the monochromaticity of the beam. This volume is often referred to as the "Coherence volume", as it is the place where the waves produce coherent EM fields. If the waves are not in phase, scattering effects do not take place, or take place to a lesser extent (depending on the degree of coherence).

The size of the coherence volume dictates the upper limit of the size of the scattering objects participating in the scattering effect. This means that attempts of detecting a structure of 1000 nanometers will not work with a coherence volume that is only 100 nanometers in the transversal directions, i.e. perpendicular to the direction of travel of the waves [Veen and Pfeiffer, 2004]. The size of the coherence volume is dependent in the transversal direction on the size of the beam-defining aperture and the distance from the aperture to the sample position (see for example the effect of a slit on the coherence volume in Figure 4, the larger the slit, the smaller the coherence volume, but the higher the intensity of the radiation). Distance from the optical element such as the slit, increases the transversal coherence length. In the longitudinal direction, the coherence length is dependent on the monochromaticity of the radiation. Polychromatic beams have small longitudinal coherence lengths [Livet, 2007].

In many X-ray experiments, the irradiated sample volume is many times the size of such a coherence volume. In these samples, many coherence volumes exist, and thus scattering occurs from each of these coherence volumes. Some experiments, however, do exploit special characteristics of scattering from a single coherent volume. These will not be discussed here, but comprehensive de-

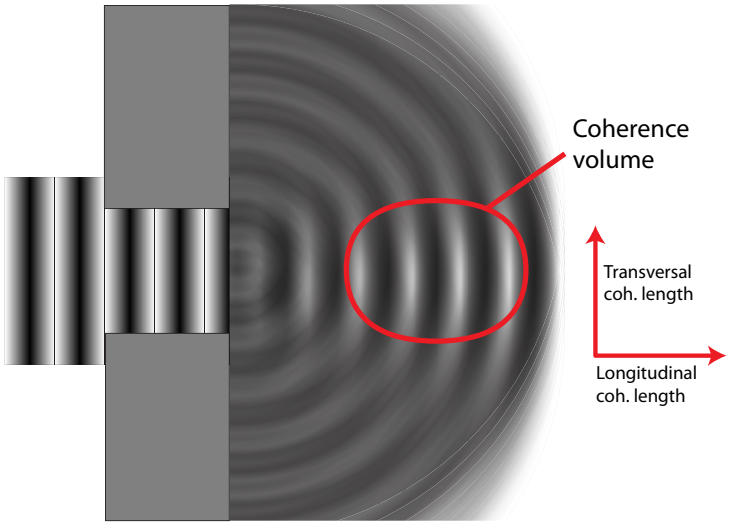

Figure 4: *Coherence volume after a slit. The larger the slit, the smaller the transversal coherence length.*

scriptions of these have been established by Livet [2007] and Veen and Pfeiffer [2004].

The EM radiation used at most SAXS beamlines mainly consists of low-energy X-rays, with a wavelength ranging from about 0.1 to several Ångström. This has only minor implications on some derivations as this restriction allows for some assumptions about the interaction between radiation and matter to be made. Most of the techniques used with X-rays, however, can be transposed onto techniques using other radiation, such as neutron sources and other techniques using EM radiation such as light scattering and vice versa.

.1.4 Many-electron systems interaction with radiation

Samples contain many electrons. The computation of the scattered amplitude from a system with many electrons can be considered as the interference (sum) of all waves emanating from each electron in the coherence volume[†].

[†]For most scattering experiments it is not strictly necessary to discuss coherence volumes, as we will not talk about coherent scattering experiments at all. However, as coherent scattering experiments become more common, it may prove useful to have touched upon the concept of coherence volumes. Additionally, it is important that the maximum size of the scatterers that can be detected by a SAXS instrument is not only limited by its geometry, but also on the coherence of the source [Veen and Pfeiffer, 2004; Livet, 2007].

The equation for the amplitude from a multitude of point sources can be written as:

$$A(\mathbf{q}) = -r_0 \sum_j \exp(i\mathbf{q}\mathbf{r_j}) \tag{9}$$

where r_0 is the Thompson scattering length if dealing with single electrons, j the index of the scattering source (electron), and $\mathbf{r_j}$ the position of the scattering centre.

For samples with continuously varying electron densities, the sum can be replaced by an integral. This makes the resulting equation into a Fourier transform function, which has great benefits for computational purposes. The scattering amplitude is the Fourier transform of the electron density difference (contrast) in the sample. The amplitude scales proportionally to the electron density contrast in the sample, the volume fractions of the phases and to the irradiated volume (c.f. Equation 13).

The Fourier transform of the electron density distribution over the correlation volume v therefore becomes:

$$A(\mathbf{q}) = -r_0 \iiint_v \rho(\mathbf{r}) \exp(i\mathbf{q}\mathbf{r}) \mathrm{d}v \tag{10}$$

.1.5 Intensity - not amplitude - is detected

In most X-ray scattering experiments, the intensity of the scattered radiation is detected, and not the amplitude. The intensity of the scattered radiation can be computed from the electron density (in each correlation volume) by calculation of the absolute square of the amplitude (as obtained from Equation 10):

$$I(\mathbf{q}) = \mid A(\mathbf{q}) \mid^2 \tag{11}$$

The scattered intensity from many correlation volumes within the sample is detected by the detector. This means that the radiation that is scattered to a certain angle is the incoherent sum of the scattering from a number N of correlation volumes in the sample [Livet, 2007], and therefore:

$$I(\mathbf{q}) = \sum_{i=1}^{N} I_i(\mathbf{q}) \tag{12}$$

The total scattered intensity for a two-phase system is proportional to Stribeck [2007]:

$$\iiint I(\mathbf{q}) d\mathbf{q} \propto V_{irr} \nu_1 \nu_2 (\rho_1 - \rho_2)^2 \tag{13}$$

where V_{irr} is the total irradiated volume, ν_i is the volume fraction of phase i and ρ_i is the electron density of phase i. This has been derived for multi-phase systems as well Ciccariello and Riello [2007].

.1.6 Small-angle X-ray scattering instruments

Overview

Three major types of small-angle scattering instruments are available today. These are the Kratky camera, which is a camera employing an X-ray beam with a line-shaped cross-section, The Bonse-Hart instrument, which uses crystals (one monochromator and one analyser crystal) to select a very small portion of the scattered beam, and finally a pinhole- or slit-collimated instrument which uses an X-ray beam with a small circular or (nearly) square cross-section. This last type of instrument is most common, and will be expanded on in detail in this chapter.

The SAXS instrument consists of several sections, each of which will be discussed in detail. A schematic picture of a three-pinhole collimated SAXS machine is shown in Figure 5. It consists of an X-ray source, a monochromator (which doubles as a focusing device), a collimation section, a sample chamber, a flight tube and a detector. In the following paragraph we will discuss each part individually.

Source

Various sources are available today for the generation of X-rays. Some of these are available as laboratory instruments, others are dedicated large-scale research facilities. We will discuss here some of the available sources.

Lab based sources started with the advent of the x-ray tube [Als-Nielsen and McMorrow, 2004]. The x-ray tube uses an electron-emitting (hot) filament cathode. The released electrons accelerate in an electric field towards the (water-cooled) anode. As the electrons hit the anode, x-rays are generated. Depending on the anode material, the characteristic wavelength of the radiation can be selected. The power of the anode is limited by the cooling method, and therefore a rotating anode has been developed. This anode consists of a rotating drum, which is water-cooled from the inside. Connecting a water-cooled drum that rotates at high speed in a vacuum chamber was one of the reasons why this type of generator only came about after the 1960's. The heat load using this

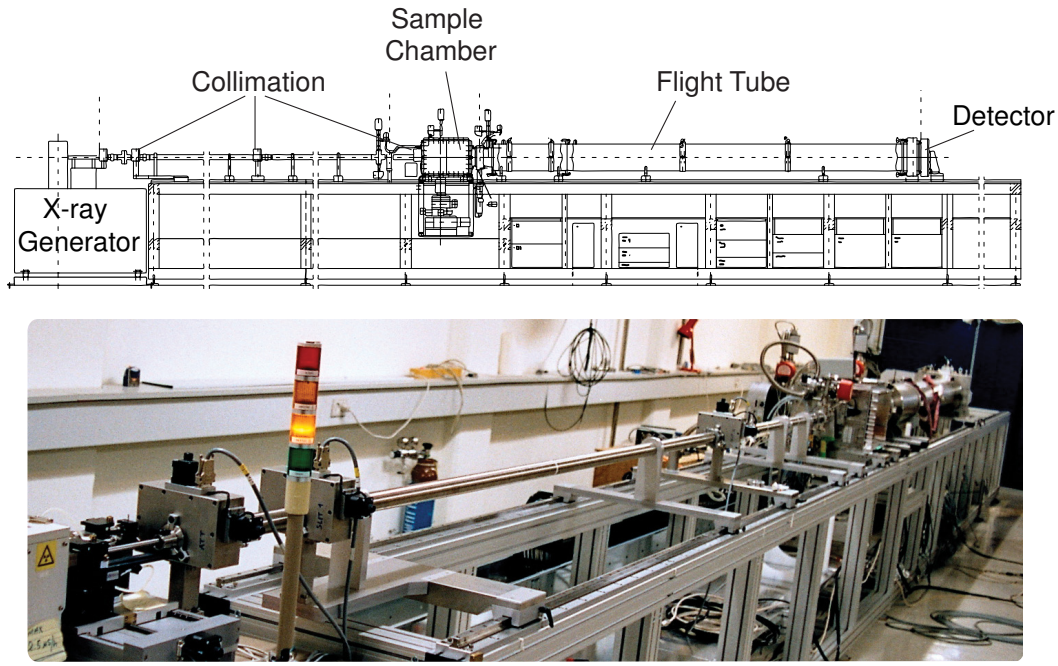

Figure 5: *Schematic depiction and photograph of the SAXS machine at DTU Risø*

drum is thus spread out over a much larger area than compared to a (static anode-based) x-ray tube, allowing for much more efficient cooling and a higher operating power (and more radiation).

Even higher intensities are obtained in particle accelerators (electron or proton) used for high-energy physics experiments. The bending magnets in those accelerators cause a deviation of the particle path, which subsequently emits radiation. The first accelerator-based x-ray experiments consisted of parasitic experiments besides the high-energy physics experiments. When it became evident that much good science could be done through the use of this radiation for (for example) materials science purposes, dedicated X-ray synchrotrons became available (sometimes as hand-me-downs from the particle physics experiments, such as the PETRA III and DORIS synchrotrons at the DESY institute in Hamburg).

Because the search for higher intensities continued, “insertion devices” such as wigglers were placed in the straight sections of the synchrotron (between the bending magnets). These bend the particle path several times in s-curves by subjecting the particle to opposing magnetic fields (thus “wiggling” the electrons). The intensity from each wiggle in a straight section can then be added. A further (and most recent) improvement was achieved by wiggling the parti-

cles just so, that the emitted wave from each wiggle would constructively interfere with the next wiggle. The intensity from two oscillations is then not two (as with the wiggler) but four times as high. These insertion devices are called undulators and are found in most modern beamlines.

Monochromatization

The source of X-rays for use in a SAXS machine has to be reasonably monochromatic, so that the required correlation length can be reached. In addition to the correlation length requirement, the accuracy of the measured scattering is also dependent on the wavelength spread, since the scattering vector $\mathbf{q}$ is dependent on the wavelength. A polychromatic beam, therefore, will smear out any scattering effects on the detector.

Several monochromatization methods exist, depending on the accuracy required. The first commonly used monochromator consists of a thin foil of metal. The absorption edges of the metal can then be used as a one-sided filter. For copper Kα radiation, for example, which commonly originates from x-ray tubes and rotating anodes which use copper as anode material, a nickel filter can be used. The monochromatization using such filters is very limited. Similarly, x-ray mirrors, which depend on the energy-dependent specular reflecting capabilities of some surfaces, can be used as a high-energy cut-off filter (as the higher the energy, the lower the required angle of incidence) [Freund, 1993].

Single-crystal monochromators are highly monochromatizing optical elements, which depend on a bragg-reflection from a crystalline material. The bragg condition of a perfect crystal is dependent on the wavelength, and thus only radiation within a certain energy window is diffracted to a selected angle. Using multiple bounces, the energy and divergence can be further fine-tuned Freund [1993]. Curved crystals can also be used for focusing the beam. Similar monochromatization and focusing effects can be achieved through fabrication of a "multilayer" mirror, which consists of many layers of deposited material, and works on the principle of bragg diffraction from stacked layers.

Collimation

Collimation of the beam is the shaping of the beam achieved through placement of various devices in the beam path. These devices usually consist of either circular pinholes in absorbing material or sets of parallel slits. Circular pinholes have the advantage that the final beam shape is circular (allowing for easier

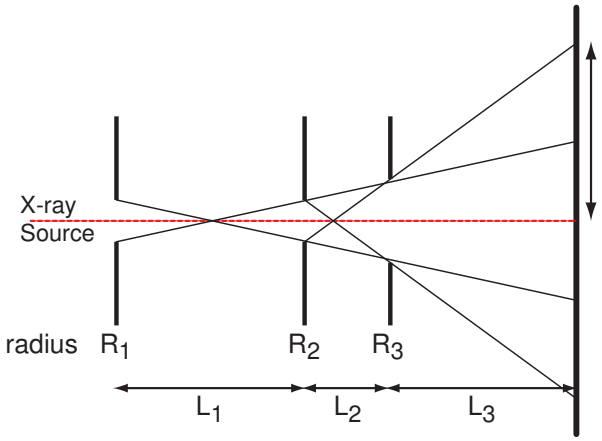

Figure 6: *Three-pinhole collimation parameters. Redrawn from [Pedersen, 2004].*

detailed data treatment), but the sizes of the pinholes are limited, and thus only a few beam sizes can be selected (depending on the number of different pinholes in the collimation system). Slit collimation creates a square beam, which is less ideal, and requires double the amount of motor drives as when pinholes are used. Slit collimation has the advantage, however, of having a near infinite number of sizes and shapes (rectangular, naturally).

For 2D SAXS purposes, a two-pinhole or two-slit collimation has often been used[‡]. The second slit, however, still introduces a considerable amount of scattering as a large amount of radiation passes the edge of the slit. This led to the introduction of a third pinhole or slit in the system, one that does not touch the primary beam, but instead only removes the scattering from the second pinhole or slit (cf. Figure 6) [Pedersen, 2004; Glatter and Kratky, 1982].

The diameter of the direct and parasitic beam scattering on the detector is related to the pinhole sizes and distances between the pinholes through [Pedersen, 2004]:

$$\Delta = R_3 + \frac{L_3(R_2 + R_3)}{L_2} \tag{14}$$

with parameters defined in 6.

[‡]1D SAXS systems sometimes work with a line-shaped beam, in a Kratky-type camera. These are very useful for measuring liquid or unoriented samples, and may also be used for measuring oriented samples, but will not be discussed here.

Sample positioning

Sample positioning is usually performed using orthogonally placed linear motor drives, i.e. one drive for motion in the horizontal direction perpendicular to the beam, and one in the vertical direction. In specific cases, however, additional alignment is required. Samples for grazing incidence and crystallography may also need rotational alignment around the three orthogonal axes (and sometimes additional translation stages are required). One new, elegant sample stage incorporating many of these motions is the hexapod or Stewart platform, consisting of a plate held aloft by six canted linear actuators [Stewart, 2009]. This plate has six degrees of freedom (3 orthogonal translations and three orthogonal rotations, with no fixed axes relative to its base plate (i.e. the centre of rotation can be defined by the user).

There are two approaches to the sample environment, evacuated chambers and air. Laboratory equipment nearly always uses evacuated chambers in which the sample is to be placed. The advantage of these is that the beam travels uninterrupted to and through the sample. The disadvantages are the increased sample mounting procedure complexity, and the limits imposed upon the sample holder dimensions as the holder needs to fit inside the vacuum chamber. For this reason, many beamlines offer sample positions in air. A wide variety of sample chambers, stretching devices, ovens and so on can be placed in this spot. The disadvantage is that there are now more objects and a volume of air in the beam path and scattered radiation path, all of which add to the background scattering.

Flight tubes

Given the length of the SAXS machine and the scattering and absorption of X-rays by air, the collimation system and the space between the sample and detector are almost always filled with vacuum tubing, although the latter tube is sometimes filled with helium instead of evacuated (this is for example done at the SLS cSAXS beamline to allow the use of a thin, large exit window). Other systems are completely evacuated, consisting of a continuous in-vacuum space [Pedersen, 2004], and thereby reducing absorption and scattering effects of x-ray transparent windows. The latter of course is the most ideal from a data collection perspective, but (as mentioned in the previous paragraph) limits are then imposed on the type of sample holders that fit within the vacuum enclosures.

Detection

X-ray detection systems depend on the transfer of energy from the x-ray photon to the detection system [Morse, 1993]. The X-ray is then either fully absorbed or fully transmitted, and therefore X-ray flight paths cannot be detected. The absorbed energy is subsequently transferred to an electrical system and then assigned to a value. The absorbed energy can be detected in four different ways (depending on the energy): by ionisation of a gas, liquid or solid, through excitation of optical states, by excitation of lattice vibrations (phonons) and through breakup of cooper pairs in superconductors. Most common for SAXS are scintillation-based and ionisation-based detection systems [Graafsma, 2009].

Detectable parameters are the photon flux, photon energy, position, arrival time and polarisation [Graafsma, 2009]. For SAXS, only the flux and position are required, and the goal of the SAXS detector is to detect these parameters with a signal-to-noise ratio which is as high as possible. The detectors can detect these parameters in four different operating modes: current (flux-) mode, integration mode, photon counting mode and energy dispersive modes. SAXS detectors commonly consist of photon counting detectors or integration-based counting detectors [Graafsma, 2009].

The two most common photon-counting detectors are wire chambers and semiconductor detectors. In the first, also known as a gas-ionisation detector, an incoming photon ionizes a gas inside the detector. The ionized particles are subsequently accelerated due to an imposed electric field, ionizing more gas along the way. Eventually the cloud of ions reaches a detector wire, causing an electrical pulse on the wire which is then detected. The intensity of the pulse is roughly related to the intensity of the incoming photon, and a coarse energy discrimination can be used to filter out (cosmic) background radiation as well as ”double” photon events. An alternative (improved) ionisation based detector is the semiconductor detector, which has a plate of semiconducting material directly accessible to X-rays. One such detector is the PILATUS detector, developed by the SLS detector group [Eikenberry *et al.*, 2003]. This detector detects photons through the change in conductivity in a semiconductor when a photon strikes. It is a low-noise photon counting system, with near-absolute position detection (only limited by the size of the pixel, as it has no point spread function like the gas-based detectors have [Né *et al.*, 1997]).

Another common type of detector is the CCD-type integrating detector. This detector commonly consists of a scintillation screen to convert the X-rays to visible light and detects this light using a commercial CCD element used in

(f.ex.) digital cameras. The advantage is that it is able to withstand much higher flux than the ionisation-based detectors, but it has significant drawbacks. It is generally not a single-photon counting device, and the obtained intensities are therefore in arbitrary units (although calibration can be done). These types are not energy discriminating, and cosmic radiation may therefore be observed. It also tends to have a drift in the gain, a high background level and relatively long readout times (which is a drawback for time-resolved experiments).

Appendix A

Bibliography

S. L. Barna, M. W. Tate, S. M. Gruner, and E. F. Eikenberry, Review of Scientific Instruments, **70**, 2927 (1999).

E. F. Eikenberry, C. Brönnimann, G. Hülsen, H. Toyokawa, R. Horisberger, B. Schmitt, C. Schulze-Briese, and T. Tomizaki, Nucl Instrum Meth A, **501**, 260 (2003).

F. Né, A. Gabriel, M. Kocsis, and T. Zemb, Journal of Applied Crystallography, **30**, 306 (1997).

C. A. Dreiss, K. S. Jack, and A. P. Parker, Journal of Applied Crystallography, **39**, 32 (2006).

G. WIGNALL and F. BATES, Journal of Applied Crystallography, **20**, 28 (1987).

F. Zhang, J. Ilavsky, G. G. Long, J. P. G. Quintana, A. J. Allen, and P. R. Jemian, Metall Mater Trans A, **41A**, 1151 (2010).

P. Boesecke and O. Diat, Journal of Applied Crystallography, **30**, 867 (1997).

The electrons usually oscillate with the same, or virtually the same frequency (also known as "elastic" interaction with the incoming radiation). There are, of course, exceptions to this ("inelastic" interactions, mentioned in a previous footnote) which can be exploited, but they go beyond the scope of this document and have therefore been omitted.

J. Als-Nielsen and D. McMorrow, *Elements of modern X-ray physics*, 2nd ed. (John Wiley & sons, 2004).

F. v. d. Veen and F. Pfeiffer, Journal of Physics- Condensed matter, **16**, 5003 (2004).

F. Livet, Acta Crystallographica Section A: Foundations of Crystallography, **63**, 87 (2007).

For most scattering experiments it is not strictly necessary to discuss coherence volumes, as we will not talk about coherent scattering experiments at all. However, as coherent scattering experiments become more common, it may prove useful to have touched upon the concept of coherence volumes. Additionally, it is important that the maximum size of the scatterers that can be detected by a SAXS instrument is not only limited by its geometry, but also on the coherence of the source [Veen and Pfeiffer, 2004; Livet, 2007].

N. Stribeck, *X-Ray Scattering of Soft Matter* (Springer-Verlag Berlin Heidelberg, 2007).

S. Ciccariello and P. Riello, Journal of Applied Crystallography, **40**, 282 (2007), three-phase samples.

A. Freund, "Neutron and synchrotron radiation for condensed matter studies," (EDP Sciences - Springer-Verlag, 1993) Chap. Chapter III- X-ray optics for synchrotron radiation, pp. 79–93.

1D SAXS systems sometimes work with a line-shaped beam, in a Kratky-type camera. These are very useful for measuring liquid or unoriented samples, and may also be used for measuring oriented samples, but will not be discussed here.

J. S. Pedersen, Journal of Applied Crystallography, **37**, 369 (2004).

O. Glatter and O. Kratky, *Small angle X-Ray Scattering* (Academic Press, 1982).

D. Stewart, Proceedings of the Institution of Mechanical Engineers Part C - Journal of Mechanical Engineering Science, **223**, 266 (2009).

J. Morse, "Neutron and synchrotron radiation for condensed matter studies," (EDP Sciences - Springer-Verlag, 1993) Chap. Chapter IV- Detectors for synchrotron radiation, pp. 95–112.

H. Graafsma, "X-ray detectors," (2009), lecture at the Nordforsk Summerschool, 2009.